Symmetry-dependent Mn-magnetism in $Al_{69.8}Pd_{12.1}Mn_{18.1}$

D. Rau, J.L. Gavilano[a], C. Beeli, J. Hinderer, E. Felder, G.A. Wigger, and H.R. Ott

Laboratorium für Festkörperphysik, ETH Zürich, 8093 Zürich, Switzerland

Abstract. We investigated the stability of magnetic moments in $Al_{69.8}Pd_{12.1}Mn_{18.1}$. This alloy exists in both, the icosahedral (i) and the decagonal (d) quasicrystalline form. The transition from the i- to the d-phase is achieved by a simple heat treatment. We present the results of measurements of the ^{27}Al NMR-response, the dc magnetic susceptibility, and the low-temperature specific heat of both phases. In the icosahedral compound, the majority of the Mn ions carries a magnetic moment. Their number is reduced by approximately a factor of two by transforming the alloy to its decagonal variety. For both compounds, we have indications for two different local environments of the Al nuclei. The first reflects a low density of states of conduction electrons and a weak coupling of the Al nuclei to the Mn-moments. The second type of environment implies a large d-electron density of states at the Fermi level and a strong coupling to the magnetic Mn moments. Spin-glass freezing transitions are observed at $T_f^{\mathrm{deca}} = 12$ K for the decagonal, and $T_f^{\mathrm{ico}} = 19$ K for the icosahedral phase.

PACS. 61.44.Br Quasicrystals – 76.60.-k Nuclear magnetic resonance and relaxation – 75.50.Lk Spin glasses and other random magnets

1 Introduction

Whether or not a transition metal ion forms a magnetic moment in a metallic matrix is a long standing problem. The first comprehensive theoretical study of the problem is due to Anderson [1]. With these Hartree-Fock-type calculations, a sharp transition between the magnetic and the non-magnetic state of the transition-metal ion was found, depending on the density of itinerant electrons, the Coulomb correlation integral, and the s-d-admixture matrix elements. The d-polarization can also severely be reduced in this model due to compensation effects [2]. In many real cases, the stability of the magnetic moment is very sensitive to small changes in the choice of the parameters. In particular in the case of Mn impurities in an Al host, it was found that the persistence of the Mn magnetic moments depends on details of the electronic structure and on the local atomic environment [3–5].

New interest in the problem of the stability of magnetic moments in metals arose with the advent of materials with nonperiodic structures, namely quasicrystals [6]. Examples of this type of solids are alloys with Al, Pd and Mn in different concentrations. Typical Al-Pd-Mn quasicrystals contain about 70% of Al and 15% of each of the transition metal elements. Related work suggests that in quasicrystals of this sort, the formation of a magnetic moment on a Mn ion depends on its position in the quasicrystalline lattice and on the local d-electron density of states at the Fermi energy $D_d(E_F)$ [7]. This scenario is supported

by the observation that in icosahedral $Al_{72.4}Pd_{20.5}Mn_{7.1}$, only a small fraction of the Mn ions carries a magnetic moment [8], and by the results of LSDA calculations, which identify the magnetic Mn ions at sites which experience a high conduction-electron density of states [9]. Previous experiments [10] showed that Al-Pd-Mn quasicrystals are either diamagnetic or only weakly paramagnetic up to Mn concentrations of 8 to 9%. The concentration of paramagnetic centers increases drastically, however, for icosahedral compounds with higher Mn content [10]. A possible reason for this observation may be the influence of mid- and long-range Mn-Mn interactions [11]. Recently, a relation between the local d-electron density of states $D_d(E_F)$ and the formation of magnetic moments on Mn ions was established experimentally by the observation of two distinct ^{27}Al NMR-lines in *decagonal* quasicrystalline $Al_{69.8}Pd_{12.1}Mn_{18.1}$, revealing two different transverse relaxations rates T_2^{-1} [12]. It was shown that the two NMR lines are due to nuclei in two different sets of environments with significantly different values of $D_d(E_F)$. The nuclei on sites with a high local value of $D_d(E_F)$ experience a strong coupling to the magnetic Mn ions, while a low local $D_d(E_F)$ provides only a weak corresponding coupling.

In this work we present the results of NMR and dc-susceptibility measurements probing the isomeric *icosahedral* compound i-$Al_{69.8}Pd_{12.1}Mn_{18.1}$. A comparison with the previous results for the decagonal compound provides evidence that d-derived extended states are formed in both types of the alloy. The effective moment per Mn ion of 2.7 ± 0.1 μ_B in the icosahedral compound is significantly

[a] e-mail: gavilano@solid.phys.ethz.ch

larger than the corresponding value of $2.1 \pm 0.1 \ \mu_B$ in the decagonal material. In the icosahedral compound nearly all the Mn atoms carry a magnetic moment, while in the decagonal compound, only about half of the Mn ions are magnetic.

2 Sample and experiment

$Al_{69.8}Pd_{12.1}Mn_{18.1}$ is the chemical composition of the stable decagonal phase in the Al-Pd-Mn phase diagram [16]. A metastable sample of i-$Al_{69.8}Pd_{12.1}Mn_{18.1}$ may, however, be obtained by spinning a melt of the material with this composition onto a fast turning (30 m/s), water-cooled Cu wheel. The resulting ribbons are 30 μm thick. They were characterized by means of selected area electron diffraction which established the high perfection of the icosahedral symmetry of the alloy. Scanning electron microscopy set the upper limit of the admixture of a second phase, i.e., $Al_{11}(Mn,Pd)_4$ on the surface of the backside of the tapes, to about 1%, and thus confirms a high chemical homogeneity of the bulk of the sample. After completion of the NMR and susceptibility measurements, the sample was exposed to the same temperature treatment as described in reference [12], in order to transform the sample into a quasicrystal with decagonal structural symmetry. The magnetic properties of the resulting decagonal material was found to be identical to those of the decagonal sample used in the work of reference [12], which was obtained in the same way from the same batch of icosahedral material. Stored at room temperature, the icosahedral compound was found to maintain its high structural quality over several years. We again emphasize that this work is an attempt to compare quasicrystalline materials of different structural symmetry but with identical stoichiometry. In this manner, the great sensitivity of the magnetic properties with respect to the Mn content is avoided. The qualities of both our materials were carefully investigated and were found to be of a standard that allows for drawing meaningful conclusions from the presented data.

The dc-susceptibility $\chi_{dc}(T)$ of i-$Al_{69.8}Pd_{12.1}Mn_{18.1}$ was measured with an rf-SQUID magnetometer between 350 K and 2 K, and in different magnetic fields ranging from 10 G to 55 kG. In view of possible spin-freezing phenomena, and in order to keep the measurement in the dc-limit, the $\chi(T)$ data-sets between 30 K and 5 K were recorded by varying the temperature very slowly, i.e., $\frac{\partial T}{\partial t} \approx 0.1 \ \mathrm{K/min}$). The freezing temperature T_f^{ico} was identified as the temperature at which irreversibility between the zero-field cooled and the field-cooled data sets in. Faster temperature variations as well as ac-susceptibility measurements (data not shown here) lead to ambiguous identifications of T_f^{ico}.

A series of NMR spectra was recorded between room temperature and T_f^{ico} in magnetic fields corresponding to the ^{27}Al resonance-frequencies of 31.2 and 66.3 MHz, using standard $\pi/2 - \tau - \pi$ spin-echo sequences. The samples were placed into a tuneable tank circuit inside a ^{4}He flow cryostat. The geometry of the resonant circuit was not changed between the measurements, thus allowing for the comparison of absolute spectral intensities if measured on the same amount of material. The precise value of the magnetic field was determined at room temperature with an aqueous solution of $AlCl_3$.

The spin-lattice relaxation rate $T_1^{-1}(T)$ was measured from room temperature down to 15 K in two different applied fields, corresponding to ^{27}Al resonant frequencies $\nu_0 = 15.5$ and $\nu_0 = 66$ MHz, respectively. The values of T_1 were extracted from fits to the nuclear magnetization recovery $m(t)$, which was first destroyed using a long comb of rf-pulses followed by a variable delay t and a spin-echo sequence $\pi/2 - \tau - \pi$ with $\tau = 180 \mu s$. We thus followed the procedure as discussed in reference [12], which allowed for a direct comparison with the results for the decagonal alloy.

The specific heat was measured by employing a thermal relaxation method, connecting the sample to a heat sink via a well-defined thermal link. The characteristic decay time of the initial temperature difference between the sample and the heat bath is a measure for the specific heat. Due to the fact that icosahedral Al-Pd-Mn is metastable, the sample could not be sintered and hence, densely packed flakes were put into a Cu container. Thermal contact was improved by adding a small amount of N-Apiezon grease which, in melted form, filled the empty space between the flakes. The background specific heat due to the Cu-container and the grease was evaluated with a separate experiment.

The electrical resistivity was measured on two polycrystalline flakes of i/d-Al-Pd-Mn, that were cut into a rectangular shape with a well-defined geometrical factor. In our four-terminal measurements, a controlled current was applied and the voltage drop across the sample was measured.

3 Experimental results

3.1 The dc-susceptibility

The main frame of Figure 1 shows the susceptibility in the form of $1/(\chi_{dc}(T) - \chi_0)$, measured in 100 G between 5 K and 300 K. The temperature independent background χ_0 was chosen to provide a Curie-Weiss type behaviour of the plotted quantity. It amounts to less than 2.5×10^{-6} (emu/mol Mn). The solid line in Figure 1 represents the Curie-Weiss part $C/(T - \Theta)$ of $(\chi_{dc}(T) - \chi_0)$. The numerical values of the essential parameters are $C = 0.924$ (emu/mol) and $\Theta = -8.2$ K. As may be seen in the upper inset of Figure 1, the field-cooled (FC) and zero-field cooled (ZFC) data-sets differ below an irreversibility temperature $T_f^{ico} \approx 19$ K. The maximum for the ZFC $\chi_{dc}(T)$ is observed at $T < T_f^{ico}$ and it is less well defined than for the decagonal sample [12] (data shown in the lower inset of Fig. 1). Nevertheless this behavior confirms a spin-glass type freezing of the Mn-moments, but via a more gradual process here than was established for the decagonal variety. The Curie constant corresponds to a
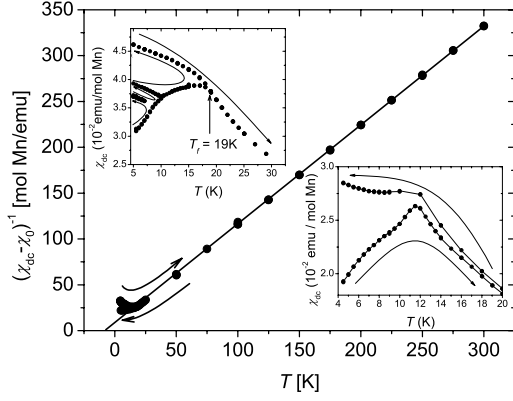
Fig. 1. The inverse dc-susceptibility $\chi(T)$ after subtracting a constant negative offset, per mol of Mn in an applied field of 100 G. The solid line represents the high-temperature Curie-Weiss fit. The upper inset displays the dc-susceptibility below 30 K in an applied field $H = 10$ G for the icosahedral alloy. The sample was cooled in zero field from room temperature down to 5 K. The field was then switched on and the temperature was varied as indicated by the arrows. Below $T_f^{\mathrm{ico}} \approx 19$ K the zero field cooled data deviates from the field cooled data. The lower inset displays the corresponding data for the decagonal compound in $H = 10$ G. The lower branch represents the zero-field cooled, the upper branch the field cooled data.

net average moment of $2.7 \pm 0.1\,\mu_{\mathrm{B}}$ per Mn atom, which is significantly larger than the $2.1 \pm 0.1\,\mu_{\mathrm{B}}$, reported for the decagonal compound.

At the lowest temperatures $\chi_{\mathrm{dc}}(T) - \chi_0$ deviates from the mentioned Curie-Weiss behavior and we plot the corresponding deviation $\Delta\chi_{\mathrm{dc}}(T)$ in Figure 2. The curve shows an increase of $\chi_{\mathrm{dc}}(T)$ with respect to the Curie-Weiss behavior with decreasing temperatures below 60 K, similar to what was found in d-$Al_{69.8}Pd_{12.1}Mn_{18.1}$, in other QCs, and in some metallic alloys containing random Mn impurities [17]. This enhancement is attributed to precursor effects of the spin-glass freezing. The inset of Figure 2 presents the same difference for the decagonal variety. In addition to the enhancement mentioned above, this data reveals a reduction of $\chi_{\mathrm{dc}}(T)$ below 100 K, reflecting the reduction of the concentration of magnetic moments discussed in reference [12]. A similar reduction does not seem to occur in the icosahedral material.

3.2 NMR spectra

In Figure 3 we compare NMR spectra for the d- and i-variety of $Al_{69.8}Pd_{12.1}Mn_{18.1}$, both recorded at room temperature and under the same conditions with an excitation frequency of 66.284 MHz. In both cases, the NMR signal is distributed over a wide range of resonant fields from 5.8 to 6.2 T. The prominent peaks near 5.98 T represent the central ^{27}Al Zeeman transition $(1/2 \leftrightarrow -1/2)$. The spectral intensity on each side of this central transition originates from the distribution of quadrupolar frequencies, a generic feature of QCs [18]. The vertical broken lines in Figure 3 indicate the maxima of the spectra.
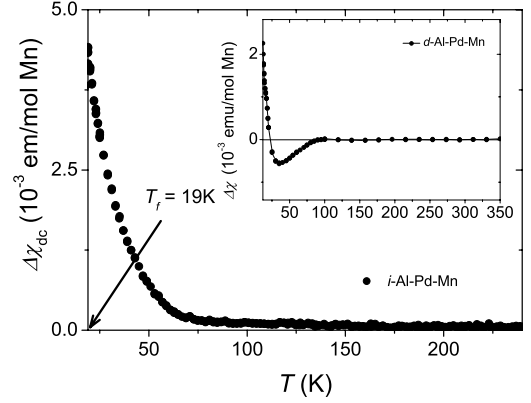

Fig. 2. Deviation $\Delta\chi(T)$ of the dc-susceptibility data from the Curie-Weiss fit to the data at elevated temperatures above 100 K. The data for the icosahedral compound in the main frame is compared with that of the decagonal material shown in the inset. Note the decrease in the data of the decagonal alloy below 100 K. This reduction of $\Delta\chi(T)$ reflects the decreasing concentration of magnetic Mn moments in the decagonal compound below $T^* \approx 100$ K, already pointed out in reference [12].
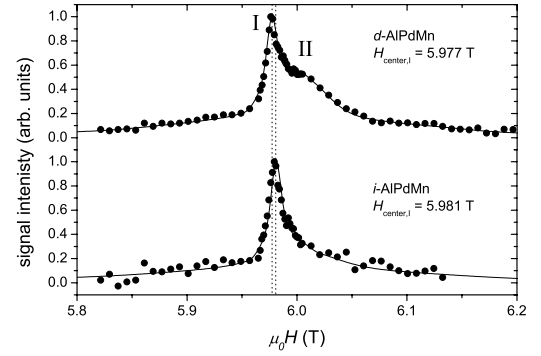

Fig. 3. NMR spectra of d-Al-Pd-Mn and i-Al-Pd-Mn at 66.284 MHz and room temperature with $\tau = 30\,\mu s$. The dotted lines indicate the position of line I. The solid lines represent the results of computer simulations of the spectra.

The solid lines represent computer simulations with fitted parameters as discussed in reference [12]. The simulations consider the quadrupolar perturbation of the central transition and the two pairs of wings of the Zeeman levels of the Al nuclei. First-order quadrupolar perturbation is considered for the wings and second order corrections for the central transition as described in standard textbooks [13]. In addition, as is common for quasicrystalline materials, a distribution of environments for the Al ions is assumed, leading to a broad distribution of quadrupolar couplings and an additional magnetic broadening of the NMR lines. This additional broadening is represented by a gaussian function and it includes the intrinsic width of the line. For more details of these simulations see [14]. For d-$Al_{69.8}Pd_{12.1}Mn_{18.1}$, the central-transition signal exhibits, in addition to the main peak at 5.977 T, a shoulder at $H \approx 6.0$ T. Additional experiments mentioned in reference [12] allowed to ascribe these features to the appearance of two lines denoted as line I and II. Line I is

associated to local Al-environments with a low conduction electron density and a weak coupling to the magnetic Mn moments and line II reflects environments with a large conduction electron density and a strong coupling to the Mn moments. Note that the shoulder corresponding to line II in d-Al$_{69.8}$Pd$_{12.1}$Mn$_{18.1}$ is absent in the ^{27}Al spectra of the icosahedral material.

Both data-sets shown in Figure 3 were measured under the same conditions, i.e., in the identical tank circuit and invoking the same number of ^{27}Al nuclei. The difference in the electrical resistivities of the two compounds is less than 10% [14] at all temperatures and, therefore, the difference in skin-depth effects are expected to be less than 5%. In addition, as mentioned before, the thickness of the samples are of the order of 30 μm, less than 5 times smaller than the corresponding skin depths under the conditions of our NMR measurements. Therefore, the ratio of the integrated spectral intensities $I_{\rm deca}^{\rm total}/I_{\rm ico}^{\rm total}$, is expected to be very close to unity. The difference of intensity due to experimental conditions is expected to be well below the uncertainty of our measurements. However, we find that $I_{\rm deca}^{\rm total}/I_{\rm ico}^{\rm total} \approx 3.4 \neq 1$, which is very close to the ratio between the total intensity of line I and II, i.e. $I_{\rm deca}^{\rm total}$, and the intensity of line I alone, i.e. $I_{\rm deca}^{\rm I}$, in the decagonal compound. In reference [12], this ratio was established to amount to $I_{\rm deca}^{\rm total}/I_{\rm deca}^{\rm I} = 3.5 \pm 0.25$ by computer fits to the spectra of the decagonal alloy. This suggests that both environments, corresponding to line I and line II, respectively, contribute to the NMR spectrum of the decagonal sample. In the spectrum of the icosahedral sample, only the intensity arising from the nuclei situated in environment I can be detected. In comparison with the data obtained for the decagonal material, the NMR-signal originating from the Al-nuclei in environment I is broader in the icosahedral compound by a factor of 2 and the temperature-independent Knight-shift of this line is larger in the icosahedral compound by a factor of 3. Contrary to our observation for the decagonal material, varying the inter-pulse separation τ had no influence on the shape of the ^{27}Al NMR spectra of the icosahedral compound, thereby adding further evidence that the spectra of i-Al$_{69.8}$Pd$_{12.1}$Mn$_{18.1}$ only reflect intensity from nuclei in one class of local environments. The nuclei that contribute to line II in the decagonal case either relax too fast to be recorded in the icosahedral alloy, or their resonance is broadened to an extent that prevents its detection with our equipment.

As opposed to the case of d-Al$_{69.8}$Pd$_{12.1}$Mn$_{18.1}$, no spectral intensity was found at any temperature in the signal of the icosahedral sample which could be attributed to non-magnetic Mn-nuclei, suggesting that in i-Al$_{69.8}$Pd$_{12.1}$Mn$_{18.1}$, most, if not all of the Mn atoms carry a magnetic moment.

3.2.1 NMR line shifts and widths

The ^{27}Al central transition line is broader for the icosahedral material than it is for the decagonal variety, and its width increases with decreasing temperature. The central
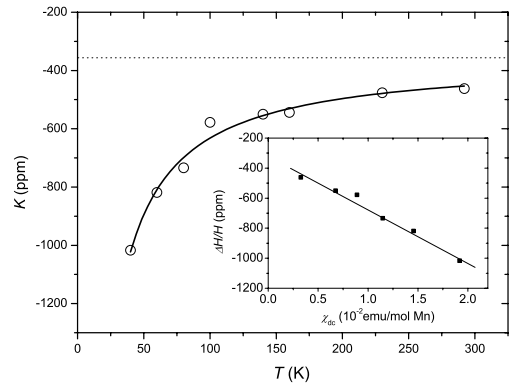

Fig. 4. ^{27}Al line shift $\Delta H/H$ for i-Al-Pd-Mn. The solid line represents a Curie-Weiss fit to the data. The dotted line indicates the constant contribution due to the Knight-shift. In the inset the same data is plotted versus the dc-susceptibility.

frequency experiences a temperature-dependent negative line-shift $\Delta H/H$ that is larger than in the decagonal alloy. Because of the larger value and the absence of line II, the shift can be decomposed according to

$$K := \frac{\Delta H}{H} = K_{\rm ce} + K_{\rm mag}, \qquad (1)$$

where $K_{\rm ce}$ denotes the temperature-independent Knight-shift, and $K_{\rm mag}$ the T-dependent shift due to the interaction of the Al-nuclei with the Mn magnetic moments. The line-shift $\Delta H/H$ was evaluated by fits employing computer simulated spectra and its temperature-dependence is displayed in Figure 4.

The constant shift $K_{\rm ce} \approx -360$ ppm, most likely due to the Pauli paramagnetism of the conduction electrons, is at least three times larger than the corresponding shift of line I but an order of magnitude smaller than that of line II in the decagonal compound. A chemical shift of this magnitude cannot be ruled out completely at this stage.

As may be seen in the inset of Figure 4, $K_{\rm mag}(T)$ varies linearly with $\chi_{\rm dc}(T)$, i.e., $K_{\rm mag}(T) = A \cdot \chi_{\rm dc}(T)$ with $A \approx -0.036$ (mol Mn/emu). Because the hyperfine coupling does not change with temperature, it is very unlikely that the concentration of magnetic Mn ions varies in a similar manner as previously observed for the decagonal alloy [12].

This conclusion is further supported by the temperature dependence of the magnetic width of line I, obtained by means of fits based on computer simulations of the spectra. The corresponding data is displayed in Figure 5. Other than the diagram shown in the inset, in which the width of the Al-line I in d-Al-Pd-Mn is plotted versus the dc-susceptibility, the width of the Al-line in i-Al-Pd-Mn reveals no sign of any change of slope in the same type of plot. The slope of the curve in the main frame of Figure 5 is 110 (G mol Mn)/(MHz emu), which is consistent with the estimated effect of a dipolar coupling of the nuclear spins of line I to the Mn moments.
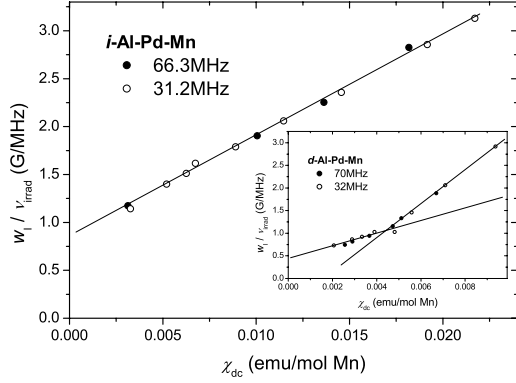
Fig. 5. Normalized magnetic width of the ^{27}Al line $w_{\mathrm{I}}/\nu_{\mathrm{irrad}}$ in i-Al-Pd-Mn. The inset shows the analogous data obtained for the decagonal sample [12].
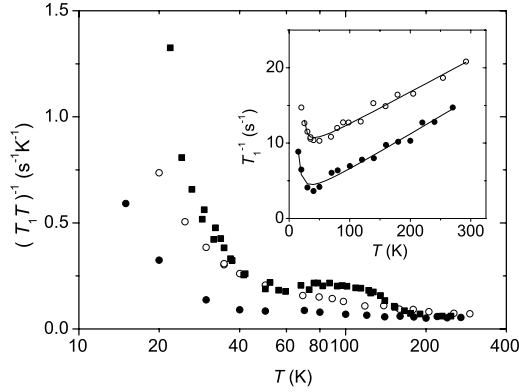

Fig. 6. Spin lattice relaxation rate in i-Al-Pd-Mn in the form of $(T_1 T)^{-1}$ versus T on semilogarithmic scales. The open and filled circles correspond to the data in the icosahedral compound measured at the frequencies 15.5 and 66 MHz, respectively. The solid squares in the main frame illustrate $T_1^{-1}(T)$ of the decagonal compound at 58 and 25 MHz. Inset: $T_1^{-1}(T)$. The lines in the inset are guides to the eye.

3.2.2 NMR Spin-lattice relaxation rate

The results for the spin-lattice relaxation rate $T_1^{-1}(T)$ are presented in Figure 6, together with the previously published data obtained for the decagonal alloy. As opposed to the spin-lattice relaxation rate in the decagonal compound, we find here that $T_1^{-1}(T)$ is strongly field-dependent across the entire covered temperature-range. $T_1^{-1}(T)$ reveals a negative slope below $T = 40$ K, and varies linearly with T above 40 K, with a positive slope of approximately 4×10^{-2} (s^{-1}K^{-1}).

It seems reasonable to decompose the spin-lattice relaxation rate into two significant contributions, such that

$$T_1^{-1} = T_{1,\mathrm{ce}}^{-1} + T_{1,\mathrm{mag}}^{-1}. \tag{2}$$

$T_{1,\mathrm{ce}}$ denotes the Korringa-type contribution due the relaxation via the conduction electrons, and $T_{1,\mathrm{mag}}$ captures the relaxation due to fluctuating Mn moments. It may be seen in the inset of Figure 6 that above 40 K, $T_1^{-1}(T)$ is

dominated by relaxation via conduction-electrons, i.e.,

$$T_{1,\mathrm{ce}}^{-1} = a \times T, \tag{3}$$

with $a \approx 4 \times 10^{-2}$ (s^{-1}K^{-1}). This value is an order of magnitude lower than for metallic Al and suggests a reduced DOS at the Fermi level due to a pseudogap in the electronic excitation spectrum. The linear temperature variation up to room temperature, on the other hand, indicates that there is no *narrow* feature in the DOS around E_F. This is distinctly different from observations, previously made in measurements of stable icosahedral Al-Pd-Mn or of highly resistive Al-Pd-Re QCs [15]. It is obvious that $T_{1,\mathrm{ce}}^{-1}$ cannot account for the total rate, however.

The other significant term in equation (2), $T_{1,\mathrm{mag}}^{-1}$, is due to the interaction between the Al nuclear spins and the fluctuating fields that originate from the Mn d-moments, which undergo a spin-glass freezing at $T_f = 19$ K. $T_{1,\mathrm{mag}}^{-1}(T)$ increases with an increasingly negative slope as T approaches the spin-glass freezing temperature T_f^{ico} but, considering the plot in the inset of Figure 6, $T_{1,\mathrm{mag}}^{-1}(T)$ is expected to be small at temperatures well above T_f^{ico}. Such a behavior is typical for nuclear spins which experience the influence of gradually slower fluctuations of magnetic moments upon decreasing temperature.

Finally, the extrapolations to $T = 0$ K of the high-temperature data recorded in two magnetic fields, displayed in the inset of Figure 6, reveal a significant temperature-independent contribution to $T_{1,\mathrm{mag}}^{-1}(T)$ even at elevated temperatures. It is inversely proportional to the applied field. No such contribution to T_1^{-1} was found for the decagonal compound. While it is not straightforward to imagine magnetic fluctuations that lead to such a behaviour, it is clear that the Mn-moment dynamics is very different for i- and d-Al$_{69.8}$Pd$_{12.1}$Mn$_{18.1}$.

4 Discussion

At temperatures above the freezing temperature T_f^{ico}, i-Al$_{69.1}$Pd$_{12.1}$Mn$_{18.1}$ reveals magnetic properties that are distinctly different from those of the decagonal variety of the same material. Although the value of the Curie temperature of the icosahedral compound is smaller by 30% ($\theta_d = -11.2$ K and $\theta_i = -8.2$ K), the spin-glass freezing temperature of the icosahedral compound significantly exceeds that of the decagonal compound. The Curie constant of the icosahedral alloy is almost twice as large as that of the decagonal material, indicating a larger effective moment per Mn ion. This is compatible with a higher concentration of moment-carrying Mn ions in the icosahedral alloy, corroborating our conclusions based on the absence of Mn spectral intensity in the NMR signal of the icosahedral compound.

The difference between the low-temperature specific heats of the icosahedral and the decagonal compound

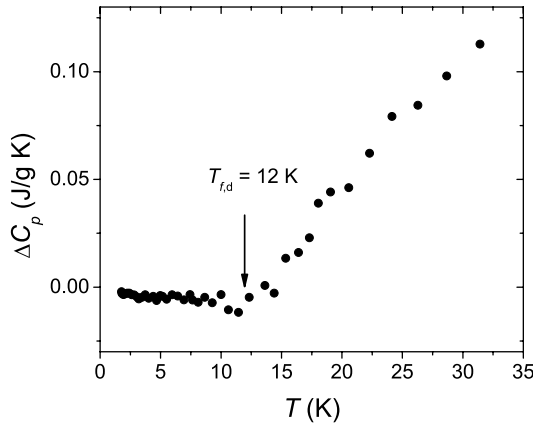$$\Delta C_p = C_p^{\mathrm{ico}} - C_p^{\mathrm{deca}} \tag{4}$$

Fig. 7. Difference $\Delta C_p = C_p^{\mathrm{ico}} - C_p^{\mathrm{deca}}$ between the low-temperature specific heats of icosahedral and decagonal $\mathrm{Al}_{69.1}\mathrm{Pd}_{12.1}\mathrm{Mn}_{18.1}$.

Fig. 8. Electrical resistivity of both alloys, scaled by the value at 0 °C, versus temperature.

is presented in Figure 7. Up to the freezing temperature of the decagonal compound $T_f^{\mathrm{deca}} = 12$ K, both quantities are equal within experimental uncertainty. Upon further heating, the icosahedral alloy releases significantly more entropy than the decagonal material. This observation suggests that the Mn moments in d-$\mathrm{Al}_{69.1}\mathrm{Pd}_{12.1}\mathrm{Mn}_{18.1}$ reveal a very similar magnetic excitation spectrum as one part of the moments in i-$\mathrm{Al}_{69.1}\mathrm{Pd}_{12.1}\mathrm{Mn}_{18.1}$. However, in the icosahedral compound, the dynamics of a second part of the moments is placed in an environment that provokes an excitation spectrum that is different from that which is valid for the decagonal compound. The corresponding additional density of states for magnetic excitations leads to a pronounced increase of the specific heat in the icosahedral alloy, exceeding that of the decagonal variety, above T_f^{deca}. They provide an additional density of states for magnetic excitations, leading to a pronounced increase of the specific heat in the icosahedral alloy, with respect to the specific heat of the decagonal variety, beyond T_f^{deca}. The gradual freezing that sets in at $T_f^{\mathrm{ico}} = 19$ K, and the field-dependence of the spin-lattice relaxation rate are most likely caused by these moments, that are only present in the icosahedral compound. The temperature-induced spin-lattice relaxation variation of decagonal $\mathrm{Al}_{69.1}\mathrm{Pd}_{12.1}\mathrm{Mn}_{18.1}$ can, apart from the anomaly at 120 K, be understood in terms of a sum of a contribution due to the conduction electrons and a term due to the interaction between the nuclear spins of Al and the Mn moments. The latter gains importance upon the gradual slowing down of the fluctuations of the Mn moments when approaching the spin-glass transition. The new data for the icosahedral compound reveals the presence of an additional field-dependent but temperature-independent background that originates from Mn moments which experience a completely different dynamics than those that are present in both, the icosahedral and the decagonal alloy.

The prefactors a of the conduction-electron contribution $T_{1,\mathrm{ce}}^{-1}$, 4×10^{-2} (s^{-1} K^{-1}) for icosahedral and 2.5×10^{-2} (s^{-1} K^{-1}) for decagonal Al-Pd-Mn, are con-

sistent with the trend of the constant contribution to the line-shift of line I, interpreted as the Knight-shift due to the conduction electrons. The latter is three times larger for the icosahedral than it is for the decagonal alloy. This indicates that the Al-sites related to line I in i-Al-Pd-Mn are exposed to a higher concentration of conduction electrons than their counterparts in d-Al-Pd-Mn. Considering that the icosahedral compound is metastable and transforms into the decagonal form upon temperature-treatment, this observation can be taken as supporting evidence for a Hume-Rothery type stabilization of the structure of quasicrystals.
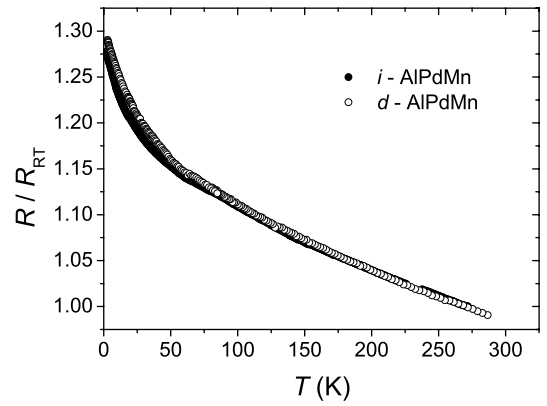
As pointed out before, K_{ce} is negative in both alloys and on both lines. Negative Knight shifts usually originate from core-polarization effects in the presence of d-type conduction electrons. Our observation therefore can be interpreted as evidence for the presence of extended d-type conduction electron states in d/i-$\mathrm{Al}_{69.1}\mathrm{Pd}_{12.1}\mathrm{Mn}_{18.1}$.

The coupling of the Al nuclei of line I to the Mn moments is, in both compounds, mainly mediated by the dipolar interaction and less so by conduction electrons. This is seen, e.g., in the slope of the curve in the width vs. susceptibility plot (Fig. 5), that is very similar for both samples above $T^* \approx 110$ K, despite the very different conduction electron densities: 110 (G mol Mn/MHz emu) for the icosahedral and 125 (G mol Mn/MHz emu) for the decagonal case. This slope is a measure for the anisotropic distribution width of the interaction between the Mn magnetic moments and the ^{27}Al nuclear spins. As mentioned in Section 3.2.1, the magnitude of the anisotropic broadening can be well explained by invoking the dipolar interaction.

The dc resistivity ratio R/R_{RT} of i-Al-Pd-Mn, displayed in Figure 8, is not field-dependent and it differs from the resistivity ratio of d-Al-Pd-Mn only insignificantly and only below 90 K. The value of the conductivities of both alloys is of equal order of magnitude. Recalling that the conduction-electron densities in the Al-environments giving rise to line I are significantly different for both alloys, other parameters than the local conduction electron density influencing line I must be important for explaining the features of the electrical conductivity.

In summary, we have probed the low-temperature magnetic properties of quasicrystalline $Al_{69.8}Pd_{12.1}Mn_{18.1}$ in both the icosahedral and the decagonal phase. As described above, the observed magnetic properties were found to be very different, although the chemical composition is the same for all our samples. Considering that repeating different measurements on a number of different samples of quasicrystalline $Al_{69.8}Pd_{12.1}Mn_{18.1}$ in both the i- and d-variety led to the same results, the observed and described differences are most likely intrinsic. We may thus conclude that our findings provide evidence for symmetry-induced changes in the low-temperature magnetic properties of quasicrystalline materials in different structural varieties but with the same chemical composition.

References

1. P.W. Anderson, Phys. Rev. **124**, 41 (1961)
2. A.M. Clogston, P.W. Anderson, Bull. Am. Phys. Soc. **6**, 124 (1961)
3. A.D. Caplin, C. Rizzuto, Phys. Rev. Lett. **21**, 746 (1968)
4. A. Narath, H.T. Weaver, Phys. Rev. Lett. **23**, 233 (1969)
5. F.T. Hedgcock, P.L. Li, Phys. Rev. B **2**, 1342 (1970)
6. D. Guenzburger, D.E. Ellis, Phys. Rev. B **49**, 6004 (1994)
7. G.T. de Laissardière, D. Mayou, Mater. Sci. Eng. **294**, 621 (2000)
8. J.L. Gavilano, D. Rau, Sh. Mushkolaj, H.R. Ott, J. Dolinšek, K. Urban, Phys. Rev. B **65**, 214202 (2002)
9. J. Hafner, M. Krajči, Phys. Rev. B **57**, 2849 (1998)
10. F. Hippert, M. Audier, J.J. Préjean, A. Sulpice, E. Lhotel, V. Simonet, Y. Calvayrac, Phys. Rev. B **68**, 134402 (2003)
11. G.T. de Laissardière, D. Mayou, Phys. Rev. Lett. **85**, 3273 (2001)
12. D. Rau, J.L. Gavilano, Sh. Mushkolaj, C. Beeli, M.A. Chernikov, H.R. Ott, Phys. Rev. B **68**, 134204 (2003)
13. G.C. Carter, L.H. Bennet, D.J. Kahan, *Metallic Shifts in NMR* (Pergamon Oxford, 1977)
14. D. Rau, Magnetism and Structure of Quasicrystals, Appendix B, Diss ETH Nr. 15415, Zurich (2004) `http://e-collection.ethbib.ethz.ch/diss/index_e.html`
15. X.-P. Tang, E.A. Hill, S.K. Wonnell, S.J. Poon, Y. Wu, Phys. Rev. Lett. **79**, 1070 (1997)
16. W. Steurer, T. Haibach, B. Zhang, C. Beeli, H.-U. Nissen, J. Phys. C **6**, 613 (1994)
17. A.F.J. Morgovnik, J.A. Mydosh, Solid State Communications **47**, 321 (1983)
18. J.L. Gavilano, B. Ambrosini, P. Vonlanthen, M.A. Chernikov, H.R. Ott, Phys. Rev. Lett. **79**, 3058 (1997)